Elsevier Editorial System(tm) for Materials Research Bulletin
Manuscript Draft

Manuscript Number: MRB-09-141

Title: Comparison of the Au nanoparticle formation and dissolution mechanisms with those of Cu and Ag nanoparticles in SiO2 sol-gel films.

Article Type: Research Paper

Section/Category: Nanomaterials

Keywords: amorphous materials, thin films , sol-gel chemistry, surface properties, optical properties.

Corresponding Author: PhD Student Jonathan Massera,

Corresponding Author's Institution: Clemson University

First Author: jonathan massera

Order of Authors: jonathan massera; Laeticia Petit; Jiyeon Choi; Martin Richardson; Yaw Obeng; Kathleen Richardson

Manuscript Region of Origin:

Abstract: This paper examines the formation and dissolution mechanisms of Au nanoparticles coinage metals in SiO2 sol-gel matrices. Using UV-Vis-NIR spectroscopy, we demonstrate that it is possible to manipulate their spatial distribution, number density and shape with a combination of light (photoexposure) and heat treatments. We show that Au nanoparticles in thin SiO2 sol-gel films can be formed at low temperature (520oC) if the annealing period is increased to 6 hours. We also demonstrate that an irradiation of the as-deposited films with an UV pulsed (Q-switched Nd:YAG) or continuous black ray UV lamp can change the number and size distribution of the Au nanoparticles. The irradiation of the films with IR femtosecond laser results in the spatially resolved

dissolution of the nanoparticles, probably due to a dramatically increased local temperature. Furthermore, we compare these mechanisms with those realized for Cu and Ag nanoparticles and we discuss the unique conditions needed to form and dissolve such Au, Cu and Ag nanoparticles and the consequences on the physico-chemical properties of the resultant films. The three different types of metallic nanoparticles have similar dissolution mechanisms induced by heat but slightly different formation mechanisms, postulated to be due to their sensitivity to oxidation. Finally, the presence of Au nanoparticles was verified using an AFM and a TA Instrument model 2990 micro-thermal analyzer (□ TA) which allows the measurement of the relative mean heat flow in the nanoparticle-doped film. The relative mean heat flow was found to increase when Au nanoparticles are formed at the surface of the films as seen previously for the Cu and Ag nanoparticle formation. We confirm that this new tool can be used as a new characterization technique to confirm the presence of Au nanoparticles in the film if located at or near the surface of the films.

Suggested Reviewers: Huidan Zeng
Shanghai Institute of Optics and Fine Mechanics,, Chinese Academy of Sciences, and Japan Science and Technology Agency
zenghuidan@yahoo.com.cn
Dr. Zeng worked on gold doped SiO2 bulk and effect of irradiation on gold nanoparticles formation. I think he is an expert on this field and can give valuable comment on this paper.

Jiawei Sheng
College of Chemical and Materials Engineering,, Zhejiang University of Technology,
shengjw@yahoo.com
Dr. Sheng worked on space selective formation of gold nanoparticles in soda-lime glasses and can give valuable comments on this paper.

Ludvik Martinu
Department of Engineering Physics, Ecole Polytechnique de Montreal
lmartinu@polymtl.ca
Dr. Martinu worked on teh effect of heavy ion beam on the deformation of gold nanoparticles. His knowledge on that field can bring interesting suggestion to improve this work.

*** New Manuscript Checklist**
Click here to view linked References

Materials Research Bulletin (MRB) New Manuscript Checklist

All new manuscripts should have the following:

☒ Text no smaller than 12 point type, double-spacing of all text pages including the references.

☒ Page numbers on each page.

☒ High quality figures, i.e. no photocopies of photographic plates, laser prints are acceptable.

☒ Large symbols used in figures, good enough for reproduction.

☒ Tables and figures at the end of the manuscript (no embedded tables/figures in text).

☒ Correct order:

-Abstract
-Introduction
-Experimental
-Results
-Discussion
-Conclusions
-References
-Tables (one table per 8½ X 11 page)
-Figure captions page
-Figures, with figure number, no caption (one figure per 8½ X 11 page)

January 23rd 2009

From:
Jonathan Massera
Advanced Materials Research Laboratory (AMRL)
Clemson University
91 Technology Drive
Anderson, SC 29625
Tel: 864-656-1259
Fax: 864-656-1099
E-mail: massera@clemson.edu

To
Editor, Materials Research Bulletin.

Dear Editor,

We, at Clemson University in collaboration with University of Central Florida, are working on the elaboration and characterization of SiO2 films with Au nanoparticles. It is important to understand how the Au nanoparticles are formed and dissolved using different heat treatment and laser exposures. Comparison with other metal nanoparticles formation/dissolution has been performed.

We are hereby submitting a manuscript titled: **Comparison of the Au nanoparticle formation and dissolution mechanisms with those of Cu and Ag nanoparticles in SiO_2 sol-gel films**, J. Massera, L. Petit, J. Choi, M. Richardson, Y. Obeng, K. Richardson.

Please feel free to contact me if you need any additional information.

Thank you for your consideration.

Sincerely yours,

Jonathan Massera

Comparison of the Au nanoparticle formation and dissolution mechanisms with those of Cu and Ag nanoparticles in SiO_2 sol-gel films.

J. Massera[1,*], L. Petit [1], J. Choi [2], M. Richardson [2],

Y. Obeng[3], K. Richardson[1]

1- *School of Materials Science and Engineering, Clemson University, COMSET, 161 Sirrine Hall, Box 340971, Clemson, SC 29634, USA*

2- *College of Optics, Center for Research and Education in Optics and Lasers (CREOL), University of Central Florida, Orlando, 4000 Central Florida Boulevard, FL 32816, USA*

3- *Nkanea Technologies Inc., 6440 Aylworth Drive, Frisco, TX 75035, USA.*

Abstract:

This paper examines the formation and dissolution mechanisms of Au nanoparticles coinage metals in SiO_2 sol-gel matrices. Using UV-Vis-NIR spectroscopy, we demonstrate that it is possible to manipulate their spatial distribution, number density and shape with a combination of light (photoexposure) and heat treatments. We show that Au nanoparticles in thin SiO_2 sol-gel films can be formed at low temperature (520°C) if the annealing period is increased to 6 hours. We also demonstrate that an irradiation of the as-deposited films with an UV pulsed (Q-switched Nd:YAG) or continuous black ray UV lamp can change the number and size distribution of the Au nanoparticles. The irradiation of the films with IR femtosecond laser results in the spatially resolved dissolution of the nanoparticles, probably due to a dramatically increased local

temperature. Furthermore, we compare these mechanisms with those realized for Cu and Ag nanoparticles and we discuss the unique conditions needed to form and dissolve such Au, Cu and Ag nanoparticles and the consequences on the physico-chemical properties of the resultant films. The three different types of metallic nanoparticles have similar dissolution mechanisms induced by heat but slightly different formation mechanisms, postulated to be due to their sensitivity to oxidation. Finally, the presence of Au nanoparticles was verified using an AFM and a TA Instrument model 2990 micro-thermal analyzer (μTA) which allows the measurement of the relative mean heat flow in the nanoparticle-doped film. The relative mean heat flow was found to increase when Au nanoparticles are formed at the surface of the films as seen previously for the Cu and Ag nanoparticle formation. We confirm that this new tool can be used as a new characterization technique to confirm the presence of Au nanoparticles in the film if located at or near the surface of the films.

Keywords: SiO_2 film, sol-gel, gold, (Au), silver, (Ag) and copper, (Cu) nanoparticles, UV/IR irradiation, micro-thermal analysis, surface roughness

1. Introduction

Small clusters of metallic atoms, commonly called nanoparticles, that have been dispersed in insulators have evolved into a new class of novel materials [1]. The ultra-fine particles and clusters of metals dispersed within dielectric media provide various non-trivial properties resulting from behavior associated with their size and their interactions with the surrounding glass matrices [2]. The metal nano-particulate centers in

these composites exhibit collective phenomena such as localized surface plasmon resonance due to the oscillations of their electrons under electromagnetic irradiation. This enables these nanoparticles to exhibit a wide range of electrical and optical properties due to the quantum size, surface and conjoint effects of the structures. The highly enhanced electromagnetic field confined around nanoparticles under an applied optical field and the significant resulting dipole moment allows for strong inter-particle interactions, which lead to their application in sub-wavelength optical energy transfer waveguides. The observed plasmon resonance spectra depend on such variables such as the nanoparticle's size, shape, local environment and density. These variables are scalable and tunable. For example, finite-difference time-domain simulations have shown direct evidence of optical pulse propagation below the diffraction limit of light along linear arrays of spherical (2D) noble metal nanoparticles with group velocities up to 0.06*c*. Interestingly, these calculations predict that a change in particle shape to spheroidal particles will result in a three-fold increase in group velocity [3].

Metal-doped organic matrices are also important; for example, platinum metal nanoparticles embedded in poly-N-vinyl-2-pyrrolidone polymer have been shown to exhibit super-paramagnetic behavior when their diameter is below 3.8 nm, as opposed to lesser paramagnetic moments in the bulk state [4]. The magnetic moment increases with decreasing particle diameter, and reaches 5.0 mB at a Pt particle diameter of 2.3 nm [4]. These observations make metal-doped nano-composites attractive as potential materials for interconnects in integrated circuits [3]. These materials also have shown potential for use as elements for optical switches [3], single electron transistors [5], matrices for data storage [6], chemical sensors, photo-catalysts [7], thermoelectric materials, optical

waveguides [8], and optical switches [9]. Until recently**,** metal-based structures have not been evaluated as optical elements due to their high reflection and absorption coefficients; however when present at the nanoscale, these metal structures can become semi-transparent due to their small size, thus, allowing them to be used as elements or components in optical applications.

Of the noble metal nanoparticles, copper (Cu) and gold (Au) nanoparticles have been extensively studied for their low bulk resistivity and their unique linear and nonlinear optical properties [9]. Copper microstructures fabricated on an indium tin oxide (ITO) substrate have shown great potential for application in optoelectronic and chemical/biological sensors [10] [11]. At the same time, matrix materials doped with gold nanoparticles have the potential to be used in the fabrication of ultra-fast all-optical switches [12], optical waveguides and waveguide lasers [13], as well as in photo-chromic media for optical disk data storage [6]. Silver (Ag) nanoparticles in silica-like films have been intensively studied over the last decade due to their multiple and diverse possible applications from antibacterial to optical applications [14].

The study of inorganic/metal nano-composite systems includes the development and optimization of the preparation techniques. These composite glasses can be fabricated using such methods as traditional melt-quenching and annealing [15], chemical vapor deposition [16], sputtering [17], ion exchange [18], and ion implantation [19]. It has been demonstrated that devices with very good optical quality and homogeneity can be obtained through a sol-gel process [20]. Here, the low temperature fabrication route afforded by sol-gel processing allows one to synthesize products that are not readily accessible by traditional melt techniques. It has been shown to be a relatively straight-

forward processing technique to form metallic nanoparticles such as Au and Ag in thermally stable oxide matrices such as SiO_2, TiO_2 [21].

Prior studies have focused on the mechanisms involved in reducing metallic ions and forming the nanoparticles in SiO_2 bulk materials [22]. In general, irradiation-assisted forming methods are attractive because of their ability to control size and density distribution of the nanoparticles [23] through controlled dose of radiation in the matrix medium. UV or visible photo-irradiation [24] and γ-irradiation methods [25] have been studied as processes promoting the formation of nanoparticles in silicate based glasses. Of particular interest was the use of excimer ultraviolet (UV) radiation to prepare fixed-size gold nanoparticles in porous silica monoliths. In this process, laser irradiation was used to control the particle sizes through a step-by-step seeding growth method [26]. It is interesting to point out that only few studies have previously focused on the spatially selective precipitation (i.e., controlled formation in specific spatial regions) of metallic nanoparticles. Hu *et al.* reported the spatially selective precipitation of Au and Ag in silicate glasses using femtosecond (fs) laser and successive annealing [27]. To the best of our knowledge, no spatially selective manipulation of coinage metal nanoparticles in sol-gel films, including but not limited to the UV and IR light assisted formation and dissolution of these metallic nanoparticles, has been previously reported.

Few authors have focused on the resulting thermal conductivity of these nanoparticles embedded in glassy matrix and on high-resolution metal line writing. We have previously leveraged radiolytic processes, initiated through multi-wavelength sources, to induce changes in nanoparticle-precursor doped SiO_2 sol-gel thin films to create spatially selective precipitation of metallic nanoparticles such as Cu [28] and Ag

[29]. We have also investigated chemical reduction via a post thermal treatment and light exposure for manipulating the physical properties of the metal nanoparticles in diverse matrices.

In this paper, we examine the processing conditions required for the formation of Au nanoparticles in SiO_2 sol-gel matrices and characterize their consequences on the physico-chemical properties of the resultant films. We show that once the metal nanoparticles are formed, it is possible to manipulate their spatial density, shapes, etc. with a combination of light and heat. We also compare the mechanisms of Au nanoparticles formation and dissolution with those of Cu and Ag nanoparticles and we discuss the unique conditions needed to form and dissolve such nanoparticles.

2. Experimental

2.1 Film deposition

Sol-gel solutions of the generalized formulation $xAu\text{-}(1\text{-}x)SiO_2$ with x=0, 0.005, 0.025 and 0.05 were prepared by the hydrolysis and condensation of high purity (98%) tetraethylorthosilicate (TEOS $C_8H_{20}O_4Si$ from Sigma Aldrich) with ethanol used as solvent. The optimal molar ratio of matrix precursor/ethanol/water/HCl was found to be 1/30/1/0.03; this formulation was used for all the experiments described in this paper. The metal precursor used was a 99.99% pure Hydrogen tetranitratoaurate (III) hydrate [$HAu(NO_3)_4\ xH_2O$ with $x\approx3$] from Alfa Aesar. Appropriate amounts of the Au precursor were dissolved in ethanol and mixed to the solution containing the TEOS; to this mixture a few drops of concentrated HCl were used as catalyst. The final solution with molar ratio of matrix precursor/ethanol/water/HCl kept at 1:30:1:0.03 was sealed in a glass container

and stirred continuously at room temperature for 24 hours in the dark, to avoid the possibility of any ambient light-induced oxidation of the gold. Finally, 15 layers of aged sol were prepared via spin-coating on pre-cleaned and dried borosilicate microscope slides; films were spun at 1000 rpm for 10 seconds. The films were then annealed at 150°C in air for 15 hours. Uniformly thick films were formed on the microscope slides; the film thickness was measured to be (600 ± 100) nm using a Zygo New View White Light Interferometer microscope.

2. 2 Light sources and experimental set up for exposure tests

The continuous wave (cw) source used during this study was a black ray lamp with a spectral bandwidth of 330 - 370nm (FWHM) around the center band of 366 nm, at a power of 2 x 6 Watt (UVL-56; UVP, LLC Co.). Doped films were irradiated using this lamp for 24 hours; the cumulative resultant dose of UV light exposure for each specimen was estimated to be ~420 J/cm^2.

The laser used for the near infrared (NIR) formation/dissolution irradiation studies was a λ=800 nm chirped-pulse amplified Ti:Al_2O_3 femtosecond laser system (Spitfire, Spectra Physics) operating at 1 kHz with the pulse duration of ~120 fs. The Gaussian laser output beam was focused using a 10X, 0.25-N.A. microscope objective at the surface of the film sample, which was translated perpendicular to the laser beam by a computer-controlled three-axis translation stage. The laser intensity was adjusted with a half-wave plate and a polarizing cube beamsplitter placed before the microscope objective. The beam size used to irradiate samples has been estimated to be approximately 4 microns.

2.3 Optical property measurements

The transmission spectra of the deposited film was measured with a dual beam UV-Vis-NIR Perkin Elmer Lambda 900 spectrophotometer at a scan rate of 2 nm/s in the 200 - 800 nm region. The measurements were performed at room temperature in ambient air. No correction for Fresnel loss has been performed.

2.4 Surface profile characterization

The film surface topography was measured using 5X and 20X objectives on a Zygo New View 6300 white light interferometer microscope (Zygo Corporation, Middlefield, CT, USA). This tool has the capability to characterize and quantify surface roughness, step heights, and other topographical features. The filter used was set to "High Pass," and the filter type set to "FFT Fixed".

2. 5 Localized Thermal Conductivity / Relative Heat flow measurements and AFM

A micro-thermal analyzer (TA Instruments (model 2990, μTA) was used to quantify local thermal conductivity of the metal particle-containing films. The system incorporates a Pt/Rh Wollaston wire probe, which functions simultaneously as both a resistive heater and resistive temperature detector (RTD). The probe was placed on an AFM head to allow high precision scanning in three dimensions. A stage temperature controlled at 27^{o}C, and a probe temperature of 127^{o}C respectively were utilized to prevent variations caused by changes in ambient conditions. This tool configuration

allows us to directly compare the results obtained using the μTA with the topographical imaging measured using an AFM.

Surface scans were conducted on three randomly selected 50 x 50 mm areas, immediately followed by an identical reference scan in air at a constant height of ~200 μm above the sample surface. These reference scans were used as non-contact reference signals for data analysis. Local relative heat flow maps were obtained by processing the scan data with ImageJ v1.63 software. The mean relative heat flow was taken from the histogram of the heat flow deviation data. The relative heat flow value after processing is a unitless quantity, but it is a (relative) indication of the differences in the local thermal properties of the nanoparticles doped films as compared to regions of films not containing metal particles [30].

The AFM measurements were performed on Dimention 3100 AFM (Veeco Inc) equipped with Nanoscope III controller. The samples were scanned by AFM operated in taping mode using silicon tips (40 N/m, MicroMasch).

3.0 Results and Discussion

The main goal of the work described in this paper is to understand the mechanism of formation and dissolution of Au nanoparticles in SiO_2 sol-gel thin films and to compare them with those of other metal coinage nanoparticles such as Cu and Ag in similar SiO_2 sol-gel matrices.

3.1 Formation of the nanoparticles

It is well known that nanoparticles can be processed in the solution prior film deposition by light-induced reduction of the metal precursor, using electron donor or after film deposition using a heat treatment in air or in reducing atmosphere with and without irradiation, depending on the nature of the nanoparticles. In the current study, the presence of the nanoparticles in the film was confirmed by measuring the absorption spectra of the glasses to identify spectral features associated with plasmon resonance features. From Mie theory [31], each nanoparticle possess a specific surface plasmon resonance absorption band who's position, intensity and absorption bandwidth can be related to the size, quantity and size distribution of the nanoparticles. In agreement with [32], the surface plasmon resonance of the Au nanoparticles exhibit bands at ~520 nm.

3.1.1 Formation of nanoparticles in the solution prior to the film deposition

For our study of the Au nanoparticles formation mechanism, sol-gel solutions were prepared with different Au precursors concentrations. Samples with the generic formulation, $xAu\text{-}(1\text{-}x)SiO_2$ (with x=0, 0.005, 0.025 and 0.05) were prepared and the optical characteristics studied as function of the dopant content. We have previously demonstrated in [28] that it is possible to form cuprous oxide (Cu_2O) nanoparticles prior to the film deposition by aging the solution in ambient light. We proposed that these nanoparticles were formed in the sol-gel solution via light induced oxidation of the dopant precursor in the solution. It is interesting to mention that no Au-based nanoparticles could be formed in the solution using this technique, suggesting that the Au precursor in the solution is more resistant to oxidation than the Cu precursor.

Figure 1 shows the transmission spectra of the investigated films after annealing as a function of gold content, x. The expected periodic variation of the transmission value as a function of wavelength seen in film spectra due to interference from the back and front surface reflections were small, due to the small thickness of the films and to the low refractive index contrast between doped films and the substrate [33]. Notice that only the transmission spectrum of the film with x = 0.05 exhibits a weak absorption band around 565 nm which can be attributed to a metallic Au surface plasmon resonance in agreement with [34] and [35]. The presence of these Au° nanoparticles in the annealed film are most likely due to the precipitation or incomplete dissolution of the Au precursor in the sol-gel solution before the film deposition.

These results contrast those previously observed in a prior study by our group [29] on Ag-doped SiO_2 sol-gel thin film prepared using the same technique as described in this paper. Unlike the observations seen here for Au-containing sols, in the silver study, no Ag nanoparticles were formed with an increase in the concentration of the Ag. In the Ag study, it was necessary to add ascorbic acid and Triton X-100 to the solution during the processing to generate Ag nanoparticles. These additions served to reduce the target metal ion and resulted in the formation of metallic particles with an average diameter of ~5nm, both in the sol and subsequently in the as-deposited films. As originally discussed by Suber *et al.* [36] and Pal *et al.* [37], ascorbic acid acts as a reducing agent, expected to facilitate the reduction of silver ions into metallic silver. Triton X-100 is believed to have formed micelles/mesoporous structures that template or confine the reactants into pores thus providing the driving force for the aggregation of nanoparticles in small aggregates. Alternatively, the ascorbic acid molecules are believed to be concentrated inside the

surfactant mesoporous structures and these aggregates reduced the Ag ions. The combination of organic reductant and surfactant were needed to create an aggregation of nanoparticles of Ag in the SiO_2 sol-gels films. It is interesting to mention that no absorption band related to Ag nanoparticles was measured in the spectrum of the film obtained from a sol-gel solution containing only Triton X-100 or ascorbic acid.

3.1.2 Formation of metallic nanoparticles after the film deposition

It is very well known that a heat treatment of metal-doped silica glass is the most effective in promoting cluster formation due to a thermally activated correlated diffusion of the metallic atoms. Miotello *et al*. have shown that an annealing in air atmosphere above 700-800^{o}C for 1 hour is the most effective means to form Au cluster in silica when gold atoms were ion-implanted [38]. Lamarre *et al.* found that a treatment at lower temperature (600^{o}C) for a longer time (2 hours) can also activate the diffusion process and consequently form nanoparticles in films [34]. In our case, the films could not be heat treated above 550^{o}C without damaging the substrate.

When heat treated in air at 550^{o}C for 6 hours, the color of the Au doped films changed from colorless to reddish, whereas no color changes were observed in similarly treated Ag- and Cu- doped films. In the case of Ag-doped thin films, we explained that during the heating of the film to 700^{o}C, a large number of the dispersed silver atoms in the SiO_2 networks oxidize to Ag_xO_y thus limiting the reduction of Ag^{+} at high temperature [29] The heating of the microscope slide at 700^{o}C has been possible due to the short heat treatment time (2 minutes). No changes of the slides' optical properties have been measured after such treatment. The absence of the Ag nanoparticles formation

when the films were heated up to 700°C or cooled down to room temperature may also be related to an increased stability of the Ag_xO_y colloids obtained by the diffusion of Na^+ into the porous SiO_2 sol-gel film [39]. We further explained in [29] that it is possible to change the color of the Ag-doped film from colorless to yellowish if the Ag-doped films are annealed for only 2 minutes in a furnace, preheated at 700°C followed by a rapid quench to room temperature. The 2 minute heat treatment at 700°C is expected to limit the amount of Na^+ diffusing into the films, hence allowing the formation of Ag nanoparticles. Figure 2 exhibits the transmission spectrum of the Au-doped film after the heat treatment in air at 550°C for 6 hours. The spectrum shows the appearance of a new band located at ~525 nm confirming the Au nanoparticles formation after the heat treatment at lower temperature for a longer treatment time. Compared to the Ag nanoparticles, Au^+ seems to be more resistant to oxidation than Ag^+ and less sensitive to Na^+ diffusion.

Also shown in figure 2 is the transmission spectrum of the film after heat treatment for 6 hours at 520°C in reducing atmosphere, such as 5% H_2 balanced Ar. The spectrum also exhibit the absorption band related to the formation of Au° nanoparticles. It is interesting to notice that i) the amplitude of this band is more pronounced and ii) its position shifts to higher wavelength when the heat treatment is performed in a reducing atmosphere. In accordance with Mie Theory [31], these variations indicate that a higher number of larger Au nanoparticles can be formed if the film is heat treated at 520°C in reducing atmosphere than in air. Similar results were obtained for the formation of Cu and Ag nanoparticles [28][29].

Many irradiation methods such as UV or visible photo-irradiation [24] and γ-irradiation methods [26] have been developed for synthesizing gold nanoparticles in various matrices. In this work, the investigated films were irradiated for 24 hours with a continuous (cw) UV lamp with a dose of 450J/cm^2 and for 30 minutes with the ns UV source with a dose of 1500 J/cm^2 followed by a heat treatment in air for 6 hours at 520^{o}C. The color of the Au-doped films changed from colorless to redish. As expected from the change of the film color, an absorption band at ~530 nm appears confirming the formation of the Au° nanoparticles in the sol-gel films as shown in figure 3. It is interesting to notice that the position and amplitude of the band depends on the UV source. The maximum of the absorption band is at 535 nm when the film was irradiated with the cw source while it shifts to 525 nm when the film was irradiated with the nanosecond laser. The amplitude of the absorption band is also higher when the film was irradiated with the ns laser source. In agreement with the Mie Theory [31], these variations of the transmission properties indicate that the ns UV exposure compared to the cw UV exposure prior to a heat treatment leads to the formation of a larger number of smaller sized Au° nanoparticles in the SiO_2 films probably due to the higher dose. During the exposure, trapped holes are released and recombined with electrons reducing Au^{3+} as described by the well known mechanism of the precipitation of metallic nanoparticles as shown in equations (1-3) below [40][41]:

$$\text{Glassy matrix} \xrightarrow{\text{Irradiation}} h^+ + e^- \qquad (1)$$

$$Au^{3+} + 3e^- \rightarrow Au(Ag)^0 \qquad (2)$$

$$nAu^0 \xrightarrow[kT]{} Au_n \qquad (3)$$

where n is the number of Au atoms congregating into Au nanoparticles, h^+ is a hole center and e^- is an electron. Due to the higher dose with the ns laser than with the cw exposure, more trapped holes are expected to be released and recombined with electrons leading to the formation of a higher number of Au nanoparticles. These experiments show that it will be possible to selectively form Au nanoparticles in specific spatial locations in SiO_2 films with controlled number, size and size distribution by performing a UV light exposure prior the heat treatment. It is interesting to mention that no coloration change related to nanoparticle formation were measured in the Cu- and Ag-doped films when performing the same experiment. This different formation mechanism for these two typees of nanoparticles might be related to the differences in oxidation of Ag^+ and/or Cu^{2+} during the irradiation and/or heat treatment probably supported by the Na^+ diffusion.

3.2 Dissolution of Metal Nanoparticles in Doped SiO_2 Sol-Gel Films

A second purpose of the study is to verify if it is also possible to dissolve the Au° nanoparticles. To the best of our knowledge, the dissolution of gold nanoparticles has never been studied in silica sol-gel thin films. Recently, we noticed that a heat treatment of films containing Cu nanoparticles leads to a partial or complete (depending on the duration and the temperature) disappearance of the nanoparticles [28]. When heat treated in air for 6 hours at 550°C, the amplitude of the absorption band at 450 and 580 nm, related to Cu° and Cu_2O nanoparticles decreases, but still remains. We also observed that the Cu° nanoparticles dissolve much slower than the Cu_2O nanoparticles; longer heat treatments are required to completely dissolve the pure Cu nanoparticles than the Cu_2O nanoparticles confirming the oxidation of Cu-based nanoparticles during heat treatment

in different steps [28]. In the case of Au and Ag nanoparticles, no dissolution of these nanoparticles could be obtained after heat treatment at 550°C for 6 hours indicating that these nanoparticles are more stable against oxidation than the Cu nanoparticles. In order to increase locally the temperature, the films containing Au nanoparticles were irradiated with a NIR fs laser with a dose of 16.8J/cm^2 and 19.2J/cm^2. As seen in figure 4, the amplitude of absorption band associated with the Au° nanoparticles decreases dramatically after the NIR fs irradiation indicating a decrease of the number of the Au° nanoparticles. The decrease of the absorption band may be due to the heating of the medium surrounding the metallic nanoparticles [42][43], to the melting of the particles [34], probably also to the oxidation of nanoparticles and/or to the generation of color centers at the focus point leading to the breaking of the nanoparticle upon the irradiating in accordance with Jiang *et al* [41]. It is expected that ultrahigh intensity of the fs laser promotes more than two-photon absorption which results in a significant increase of the local temperature at the focus point of the laser, driving the conversion of nanoparticles into ions or individual atoms. This may result in the spatially resolved dissolution of the Au° nanoparticle in thin sol-gel films. Similar dissolution mechanism of the Ag° nanoparticles has also been observed [29].

3.3 Resulting morphology of the metal-doped sol-gel SiO_2 films

Atomic Force Microscopy (AFM) was used to investigate the surface morphology and to follow the formation of metal nanoparticles in these films. After the film was annealed in air or irradiated using the cw source, the surface morphology changes with an increase of the RMS roughness to ~(27±5) nm and ~(34±5) nm, respectively. As seen in

the figure 5, after the heat treatment in air, gold nanoparticles with diameter between 30 and 60nm can be seen clearly. Their diameter increases between 40 and 80 nm when the film is irradiated with the cw UV light prior to the heat treatment. This change of nanoparticles diameter is in accordance with the position of the absorption band related to the Au nanoparticles which was measured at 525 nm when the film is heat treated in air (figure 2) and at 535 nm if the film is irradiated with a cw UV source prior to the heat treatment (Figure 3). In agreement with the Mie Theory [31], the red-shift of this absorption band can be related to larger nanoparticles. The increase of the film roughness measured with the Zygo white light interferometer microscope with the formation of Au nanoparticles is in agreement with our previous studies [28][29]. Further TEM analysis of the films needs to be investigated to complement the AFM micrographs.

3.4 Thermal characteristics of the metal-doped sol-gel SiO_2 films

It is expected that a film containing metal nanoparticles would have a higher thermal conductivity than corresponding sample without nanoparticles [42]. We have developed a new technique for characterizing the thermal properties of the metal-doped sol-gel films [30]. The new technique relies on the measurement of the micro-thermal conductivity, which is directly proportional to the relative mean local heat flow. Using a micro-thermal analyzer from TA instrument, we demonstrated that the formation of the Ag and Cu nanoparticles can be confirmed by measuring an increase of the mean heat flow if the Cu or Ag nanoparticles are located at the surface of the films [28][29]. Figures 6a to d present the relative heat flow map of a film with $x = 0.025$ before and after heat treatment in air, in H_2 and UV light exposure prior to heat treatment in air, respectively.

The mean relative heat flow increases slightly from (~0.13 ± 0.01) to (~0.15 ± 0.01) as soon as few Au nanoparticles are formed. However, no further changes in the relative heat flow are observed when the films are subjected to various thermal anneals. Since the probe only samples the surface of the film, it is conceivable that we could not detect the nanoparticles beyond the sampling range of the probe. This would be consistent with the AFM data that seem to suggest that only the tips of the Au° nanoparticles protrude through the film / air interface when the film was pre-seasoned with irradiation before thermal anneal. Thus, notwithstanding the sampling volume limitation, the micro-thermal analyzer can resolve the presence of metal nanoparticles dispersed in dielectric matrices. However, this technique does not seem to provide information related to the number of the nanoparticles if they are not located on the surface.

4.0 Summary and future laser processing (line writing) of resulting films

The data we have accumulated so far appears to suggest that the growth mechanism of different metal nanoparticles such as Cu, Ag and Au are different for each metal. In our work, we report on efforts to elucidate the mechanism of formation and dissolution of these different metallic nanoparticles. While the preliminary results summarized in this paper provide some insight into Au nanoparticle formation and dissolution mechanisms in SiO_2 sol-gel thin films, several important questions remain which need to be answered. For example, can the partial or complete replacement of SiO_2 by other glassy matrices lead to an improvement in nanoparticle formation and/or dissolution? The matrices we have studied to date are based on SiO_2, but we intend to extend to other oxide and possibly non-oxide matrices formed via a sol-gel solution as

found in more recent reports. For example Rivallin *et al*. [45] studied the temperature dependence of TiO_2 sol precipitation kinetics in the sol-gel method using titanium isopropoxide, while Jing *et al.* [46] investigated the fabrication and characterization of GeO_2 film using tetraethylorthogermanate and Lecomte *et al.* [47] have reported on the sol-gel processing of TeO_2 films using tellurium isopropoxide as a precursor. Since these three oxide matrices are good candidates for film deposition via a sol-gel route, their optimization by adding or replacing the SiO_2 matrix with TiO_2 and/or GeO_2 or TeO_2 will be studied, to compare the efficiency in generating metallic nanoparticles under light exposure. In the case of non-oxide glass it has been found that it is difficult to obtain films using a sol-gel technique. Chern and Lauks first introduced the spin-coating deposition method of preparing chalcogenide films in 1982 [48]. They demonstrated that amorphous chalcogenide films can be deposited from their solutions and retain many of the solute properties. Subsequent to these initial efforts, several groups have extended efforts to produce spin-coated chalcogenide films of As_2S_3, As_2Se_3 and Sb_2S_3 [49] [50]. However a lack of data on the formation/dissolution of metal nanoparticles in such matrices has been evidenced. Thus, the deposition of new chalcogenide film with metal nanoparticles will be investigated using a metal nanoparticles doped chalcogenide glass or an undoped chalcogenide glass dissolved in a solution containing metal nanoparticles.

References

1. W.P. Halperin, Rev. Mod. Phys., 58 (1986) 533

2. P. Jena, S.N. Khanna, B.K. Rao, Journal of Cluster Science, 12 (2001) 443–456

3. S. A. Maier, P.G. Kik, H.A. Atwater, Physical Review B 67 (2003) 205402.

4. Y. Yamamoto, T. Miura, Y. Nakae, T. Teranishi, M. Miyake, H. Hori, Physica B 329–333 (2003) 1183–1184

5. A. Nakajima, H. Nakao, H. Ueno, T. Futatsugi, N. Yokoyama, Appl. Phys. Lett. 73 (1998) 1071

6. X.G. Huang, M.R. Wang, Y. Tsui, C. Wu, Journal of Applied Physics, 83 (1998) 3795

7. A. D. Zamkovets, S.M. Kachan, A.N. Ponyavina, N.I. Sil'vanovich, J. Appl. Spectroscopy, 70 (4) (2003) 593-598

8. M. Frumar, T. Wagner, Current Opinion in Solid State & Materials Science, 7 (2003) 117

9. H. Inouye, K. Tanaka, I. Tanahashi, K. Hirao, Physical Review B, 57 (1998) 11334, (1998).

10. R. Bhattacharya, P. Mukherjee, Advanced Drug Delivery Reviews, 60 (2008) 1289-1306.

11. P.K.H. Ho, M. Granstrom, R.H. Friend, N.C. Greenham, Advanced Materials, 10 (1998) 769

12. N.F. Borrelli, D.W Hall, D.R Ulhmann, N.J. Kreidl (Eds.), Optical Properties of Glass, American Ceramic Society, Westerville, OH (1991) 87

13. A. Polman, D.C. Jacobson, D.J. Eaglesham, R.C. Kistle, J.M. Poate, Journal of Applied Physics, 70 (1998) 3778

14. F. Gonella, Nucl. Instrum. Methods B 166-167 (2000) 831

15. Valentin E., Bernas H., Ricolleau C., Creuzet F., Phys. Rev. Lett., 86 (2001) 99

16. M. Dublel, G.Mosel, Journal of Applied Physics Part 1, 33 (1994) 5892

17. Y. Maeda, Physical Review B, 51 (1995) 1658

18. Y. Hamana, N. Hayahsi, A. Nakamura, S. Omi, Journal of Luminescence, 87 (2000) 859.

19. F. Gonella, G. Mattei, P. Mazzoldi, C. Sada, G. Battaglin, E. Cattaruzza, Applied Physics Letters, 75 (1999) 55

20. T. Lutz, C. Estournes, J.C. Merle, J.L. Guille, Journal of Alloys and Compounds, 262-263 (1997) 438-442

21. U. Schubert, New J. Chem, 18 (1994) 1049

22. H. Zeng, J. Qiu, X. Jiang, C. Zhu, F. Gan, Journal of Crystal Growth, 262 (2004) 255

23. X. Jiang, J. Qiu, H. Zeng, C. Zhu, K. Hirao, Chemical Physics Letters, 391 (2004) 91-94

24. K. Esumi, K. Matsuhisha, K. Torigoe, Langmuir, 11 (1995) 3285

25. K. Malone, S. Weaver, D. Taylor, H. Cheng, K.P. Sarathy, G. Mills, Journal of Physical Chemistry B, 106 (2002) 7422

26. A. Heinglein, D. Meisel, Langmuir, 14 (1998) 7392

27. X. Hu, Q. Zhao, X. Jiang, C. Zhu, J. Qiu, Solid State Communications, 138 (2006) 43

28. J. Massera, J. Choi, L. Petit, M. Richardson, Y. Obeng and K. Richardson, Materials Research Bulletin 43, (11) (2008) 3130-3139

29. J. Massera, A. Martin, J. Choi, T. Anderson, L. Petit, M. Richardson, Y. Obeng, K. Richardson, submitted to Journal of Physics and Chemistry (submission: April 10, 2008)

30. N. Carlie, J. Massera, L. Petit, C. Vigreux-Bercovici, A. Pradel, K. Richardson, submitted to Rev. Sci. Instrum. (submission: December, 2008)

31. G. Mie, Annals of Physics, 25 (1908) 377

32. L.B Scaffardi, N. Pellegri, O. de Sanctis, J.O. Tocho, Nanotechnology, **16** (2003) 158,

33. R. Swanepoel, Journal of Physics E: Scientific Instruments, 16 (1983) 1214

34. J-M. Lamarre, Z. Yu, C. Harkati, S. Roorda, L. Martinu, Thin Solid films, 479 (2005) 232-237

35. H. Zeng, J. Qiu, Z. Ye, C. Zhu, F. Gan, Journal of Crystal Growth, 267 (2004) 156-160

36. L. Suber, I. Sondi, E. Matijevic, D.V. Goia, J. of Colloid and Interface Science, 288 (2005) 489.

37. A. Pal, T. Pal, Journal of Raman spectroscopy, 30 (1999) 199.

38. A. Miotello, G. De Marchi, G. Mattei, P. Mazzoldi, C. Sada, Physical Review B, 63 (2001) 5409

39. M. Mennig, M. Schmidt, H. Schmidt, J. Sol-Gel Technol. 8 (1997) 1035

40. J. Sheng, K. Kadono, T. Yazawa, Journal of Non-Crystalline Solids, 324 (2003) 295-299

41. X. Jiang, J. Qiu, H. Zeng, C. Zhu, Journal of Materials Research, 18 (2003) 2097-2100

42. S. Lefevre, S. Volz, J. Saulier, C. Fuentes, Review of Scientific Instrument, 74 (2003) 2418-2423

43. J.H. Hodak, A. Henglein, G.V. Hartland, Journal of Physical Chemistry B, 104 (2000) 9954

45. M. Rivallin, M. Benmami, A. Gaunand, A. Kanaev, Chemistry Physics Letters, 398 (2004) 157

46. C. Jing, J. Hou, X. Xu, Optical Materials 30 (2008) 857–864

47. A. Lecomte, F. Bamiere, S. Coste, P. Thomas, J.C. Champarnaud-Mesjard, Journal of the European Ceramic Society, 27 (2007) 1151-1158

48. G. C. Chern and I. Lauks, J. Appl. Physics. 53, 6979 (1982).

49. B. Singh, G. C. Chern and I. Luaks, Appl. Phys. Lett. **45**, 74 (1984).

50. E. Hajto, P. J. S. Ewen, R. E. Belford and A. E. Owen, Thin Solid Films **200**, 229 (1991).

Figures caption

Figure 1: Transmission spectra of Au doped SiO_2films prepared with x = 0, 0.005, 0.025 and 0.05 (a). (b) is the zoom in to exhibit the probable absorption band at 565nm in the spectrum of the glass with x = 0.05 and small interferences for the other spectra

Figure 2: Transmission spectra of a film with x = 0.025 after heat treatment in air and in reducing atmospheres at 520^{o}C for 6 hours.

Figure 3: Transmission spectra of a film with x = 0.025 after irradiation using cw and ns UV source followed by a heat treatment in air at 520^{o}C for 6 hours.

Figure 4: Transmission spectra of a film with x = 0.025 containing Au nanoparticles before and after fs laser irradiation

Figure 5: Atomic Force Microscopy images of Au doped film with x = 0.025 after deposition (a), heat treatment in air (b) and after irradiation using cw followed by heat treatment in air (c).

Figure 6: Map of the relative heat flow (Q) for a film with x = 0.025 after deposition (a), heat treatment in air (b) heat treatment in H_2 (c) and UV light exposure prior to heat treatment in air (d)

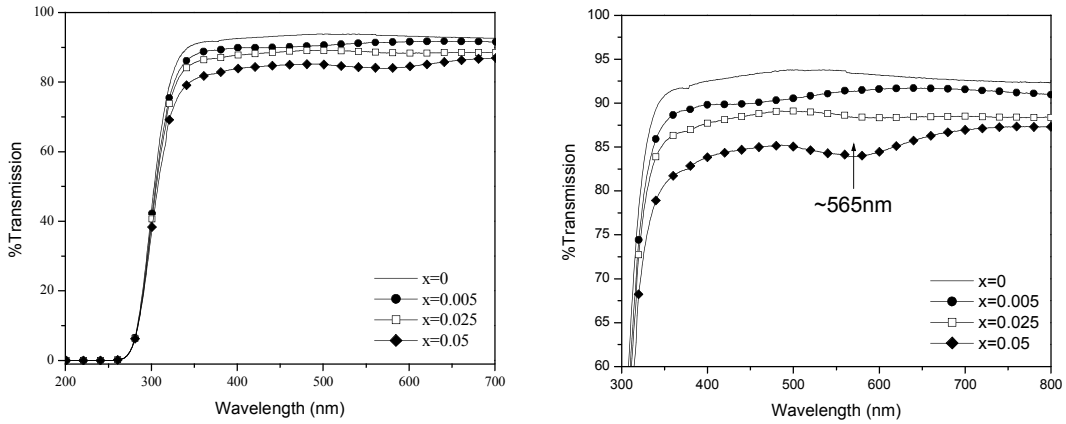

a) b)

Figure 1

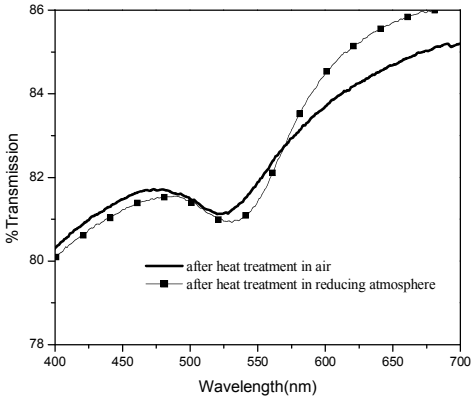
86
84
82
80
78
% Transmission
400
450
500
550
600
650
700
Wavelength(nm)
after heat treatment in air
after heat treatment in reducing atmosphere

Figure 2

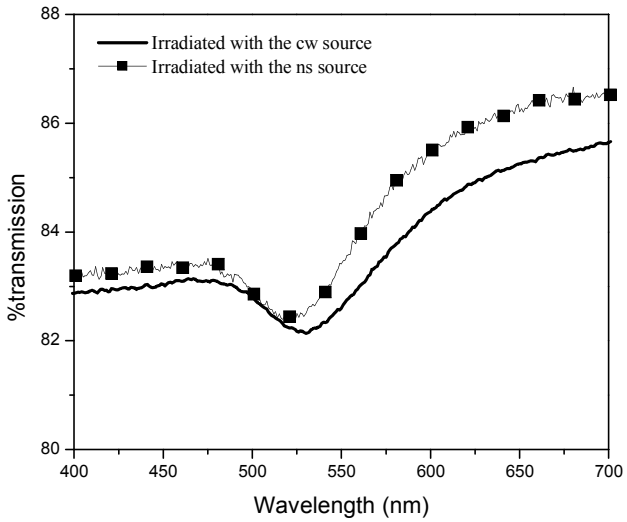
Irradiated with the cw source
Irradiated with the ns source
%transmission
Wavelength (nm)
88
86
84
82
80
400
450
500
550
600
650
700

figure 3

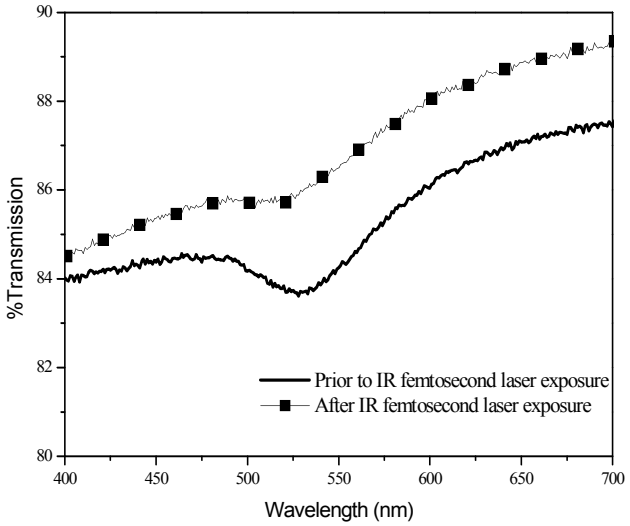
90
88
86
84
82
80
%Transmission
400
450
500
550
600
650
700
Wavelength (nm)
Prior to IR femtosecond laser exposure
After IR femtosecond laser exposure

figure 4

a) b) c)

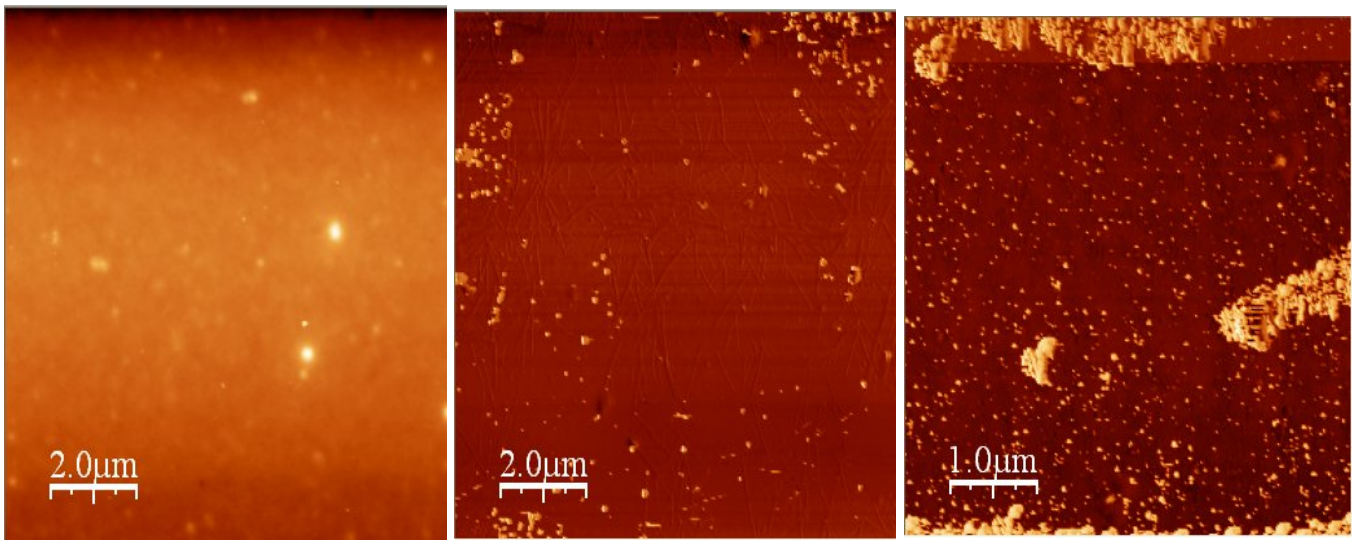

figure 5

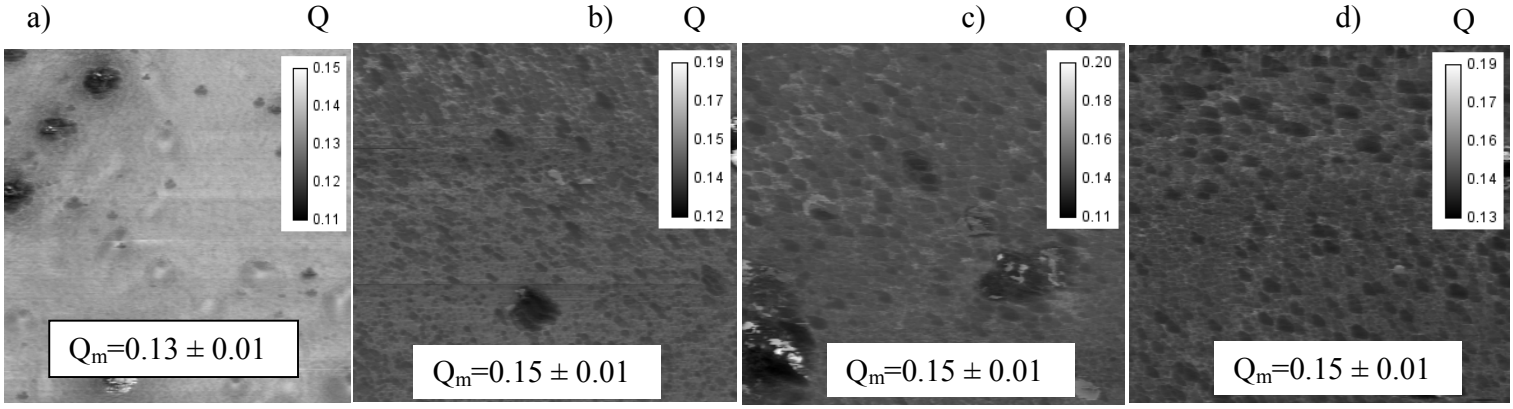
a)
Q
0.15
0.14
0.13
0.12
0.11
Q_m=0.13 ± 0.01
b)
Q
0.19
0.17
0.15
0.14
0.12
Q_m=0.15 ± 0.01
c)
Q
0.20
0.18
0.16
0.14
0.11
Q_m=0.15 ± 0.01
d)
Q
0.19
0.17
0.16
0.14
0.13
Q_m=0.15 ± 0.01

Figure 6